Volume I N° 4

Revue de l'Entrepreneuriat et de l'Innovation

Development of a new biosorbent based on the extract residue of marine alga Sargassum vulgare: application in biosorption of heavy metals

Meriem Tarbaoui [1*], Mina Oumam [2], Mourad Benzina [3], Ahmed Bennamara [1], Abdelmjid Abourriche [1]

[1] *Laboratoire Biomolécules et Synthèse Organique (BioSynthO), Faculté des Sciences Ben M'Sik, Université Hassan II de Casablanca, Maroc.*

[2] *Laboratoire d'Ingénierie des Matériaux, Faculté des Sciences Ben M'Sik, Université Hassan II de Casablanca, Maroc.*

[3] *Laboratoire Eau, Energie et Environnement, Ecole Nationale d'ingénieurs de Sfax, Université de sfax, Tunisie.*

**Corresponding Author. E-mail: meriem_tarbaoui@yahoo.fr; Tel: (+212660387289)*

Abstract- In the present work, we conducted research in order to study the possibility of producing a new biosorbent from a sub-product of seaweed; it is the extract residue of the marine alga Sargassum vulgare, which represents more than 80% by weight of the raw material. It is a natural residue that we could turn into biosorbent under the effect of chemical activation with phosphoric acid which allows the development of a large pore in the activated material. To optimize the conditions for elaboration of our biosorbent, experimental design was applied to reduce the number of experiment trials needed to evaluate some parameters (percentage of phosphoric acid, temperature and time of activation) and their effects on the responses (capacity of biosorption of methylene blue, yield biosorbent). The product obtained under the optimal conditions has good textural and structural properties and developed surface functions. The application of optimized biosorbent in the removal of some heavy metals (Pb(II), Cu(II), and Cd(II)) from aqueous solutions was studied. The impact of various parameters such as pH, biosorbent dose, and contact time on the removal was evaluated by batch method. The biosorption isotherms were studied using Langmuir, Freundlich, Dubinin–Radushkevich (D–R), and Temkin isotherm models. Langmuir isotherm provided the best fit to the equilibrium data. The experiments demonstrated that the removal of metal ions followed the pseudo-second-order kinetic model. Desorption experiments were carried out using HCl solution with a view to regenerate the spent biosorbent and to recover the adsorbed metal ions.

Keywords: Biosorbent, Marine alga, Sargassum vulgare, Biosorption, Heavy metals, Biosorption isotherms, Biosorption kinetics, Desorption.

I. INTRODUCTION

Control of toxic metal pollution is becoming increasingly important as industrialization becomes the main economic activity of many nations. Heavy metals, including cadmium (Cd), chromium (Cr), copper (Cu) and lead (Pb) are among the most important of such pollutants because of their toxicity and non-biodegradability [1-3]. Biosorption is an innovative technology that employs inactive and dead biomass for the recovery of heavy metals from aqueous solutions. As an alternative to traditional methods, its promising results are now being considered for application by the scientific community. In this context, research and development of new biosorbent materials has focused especially on algae, due to its high sorption capacity and its availability in almost unlimited amounts [4]. The objective of this study is the valorization of the part not extractible of marine alga by the development of a new biosorbent, optimization of conditions for its preparation, their characterization, and its application in the biosorption of heavy metals. The influence of various parameters such as pH, contact time, and biosorbent dose on the removal efficiency of the biosorbent was studied. The kinetics of metal ions biosorption onto the biosorbent was analyzed by kinetic models. The experimental equilibrium biosorption data were analyzed by Freundlich, Langmuir, Dubinin Radushkevich, and Temkin isotherm models to determine the best fit isotherm equation. Desorption experiments were carried out using HCl solution.

II. MATERIALS AND METHOD

II.1. Biomass and chemical modification

The algae used in this study were collected from the Dar Bouaaza beach (Casablanca), Morocco in June 2011. Prior to extraction, the marine algae were identified, washed with running water and with deionized water. The washed biomass was oven-dried at 60 °C for 24 h, ground using an electric grinder, and extracted by methanol In order to eliminate the maximum of the extractable organic matter. The extract residues of the algae were washed with double distilled water, dried at 110 °C for 24 h, ground and reduced to a particle size between 1 and 2 mm, the obtained material was mixed with phosphoric acid (H_3PO_4), with a weight ratio of phosphric acid/ obtained material equal to 1/1. The mixture was dried overnight at 120 °C. The activated product has subsequently undergone heat treatment in air. The domains of variation of activation temperature, activation time and percentage of chemical activated agent were defined on the univariate analysis. To optimize the conditions for the elaboration of our biosorbent, the methodology of experimental design was used to reduce the number of experimental trials necessary for evaluation of the parameters studied (percentage of phosphoric acid, activation temperature and activation time) and their effects on the responses (biosorption capacity of methylene blue and yield biosorbent). The optimised biosorbent was obtained using 225°C activation temperature, 150 min activation time and 70% of chemical activating agent, resulting in 66.14% of mass yield and 93.77 % of methylene blue biosorption capacity [5]. The optimised biosorbent was washed with distilled water until all acid was eliminated, dried, ground and sifted to obtain a powder with a particle size capable of passing through a 100µm sieve; it was finally kept in a hermetic bottle for subsequent uses.

II.2. Physico-chemical characteristics of the biosorbent

II.2.1. Porosity and pore volume

The porosity and pore volume of the biosorbent were given by pycnometry. In order to determine the real density (ρ_s), water was chosen since it can penetrate in porous space [6]. Whereas, for the apparent density (ρ_p), mercury was chosen since it does not penetrate in the porous network. The porosity (χ) and pore volume (V_P) can be calculated by following equation:

$$X = \frac{\rho_s - \rho_p}{\rho_s} \times 100 \quad (1)$$

$$V_P(g/cm^3) = \frac{1}{\rho_p} - \frac{1}{\rho_s} = \frac{\chi}{\rho_p} \quad (2)$$

II.2.2. Surface area evaluation

The specific surface area of the biosorbent was estimated by the methylene blue (MB) biosorption method. MB stock solution 1000 mg/L was prepared by dissolving 1 g of MB in 1000 mL of deionized water. In a series of 250 mL glass bottles were placed successively 100 mL of MB solutions with initial concentration varying between 100 and 1000 mg/L and a biosorbent dose of 4 g/L. The bottles were capped and shaken for 24 h in a thermostatic bath at 25°C until biosorption equilibrium was established. Samples were taken and centrifuged at 4000 rpm and the supernatant was analyzed by measuring the absorbance at 664 nm, using a UV–visible spectrophotometer [7]. The amount of MB biosorbed q (mg/g biosorbent) was calculated by using the equation:

$$q = (C_0 - C_e)\frac{V}{m} \quad (3)$$

where C_o and C_e are the initial and equilibrium MB concentrations, respectively (mg/L), V is the

total volume of the suspension (L), and m the biosorbent dose (g). The plot of 1/q versus $1/C_e$ for the biosorption of MB on the biosorbent gave the saturation biosorption amount, determined from the slope of the plot. The MB molecule has a parallelepiped shape and can be regarded as a rectangular volume with dimensions 17 × 7.6 × 3.25 Å. Previous research reported that, generally, for monolayer biosorption 2.45 m2 can be taken as the occupying area for 1 mg MB. The specific area of the biosorbent was calculated by using the equation:

$$S = 2{,}45 \times Q_m \qquad (4)$$

II.2.3. Iodine number

The iodine number (mg/g of biosorbent) was evaluated using the procedure proposed by the Standard Test Method (ASTM D 4607-86). The biosorbent (approximately 0.3–0.6 g) was placed in a 250 mL dry Erlenmeyer flask, and was fully wetted with 10 mL HCl 5% (in weight). The mixture was then boiled for 30 s and finally cooled. Then 100 mL of iodine solution (0.1 M) was poured into the flask, and the mixture was vigorously shaken for 30 s. After a quick filtration, 50 mL of the solution was titrated with sodium thiosulfate (0.1 M) until the solution became pale yellow. Two milliliters of starch indicator solution (1 g/L) were added, and the titration was continued with sodium thiosulfate until the solution became colorless. The concentration of iodine in the solution was thus calculated from the total volume of sodium thiosulfate used.

II.2.4. pH of contact

The measurement of pH of contact can quickly evaluate the acidity or basicity of a biosorbent. It was carried out and measured as follows: 50 mg of the biosorbent was placed in a 250 ml vessel and 100 ml of deionised water was added. This mixture was agitated for 24 h and filtered. The pH of residual solution was measured using pH-metter [8].

II.2.5. pH Point of zero charge (pHPZC)

The pH of zero point of charge (pHzpc) was determined by adding a known amount of the biosorbent (0.1 g) to a series of bottles that contained 50 mL of deionised water. Before adding the biosorbent, the pH of the solutions was adjusted to be in the range of 1.0–9.0 by the addition of either 0.1 M HCl or 0.1 M NaOH. These bottles were then rotated for 1 h in a shaker and pH values were measured at the end of the test. The pH of the suspensions is represented as a function of the initial pH of the solutions. The curve obtained theoretically cross the bisector of axes at the point of zero charge [9].

II.2.6. Fourier transform infrared (FTIR) spectroscopy

FTIR was principally employed as a qualitative technique for the assessment of the chemical structure of biosorbent. The FTIR spectra of the resulting biosorbent were recorded between 400 and 4000 cm-1 in a spectrometer type Perkin-Elmer 783.

II.2.7. Surface functional groups

The well-known Boehm's method allows modeling the principal acidic oxygenated functions of the biosorbent such as carboxylic acids, lactones, and phenols using bases of increasing strength as NaHCO3, Na2CO3 and NaOH, respectively. Then, the total basicity is given by titration by HCl [10-11].

II.2.8. X-Ray diffraction

The X-Ray diffraction patterns were obtained using a PANalytical diffractometer equipped with a CuKα radiation (45 kV, 40 mA) at a step size of 0.06º between 5 and 90º.

II.2.9. Surface morphology

Scanning Electron Microscopy (SEM) was employed to visualize the external morphology.

In the present work, the raw material and the prepared biosorbent were analyzed by this technique using Environmental Scanning Electron Microscope (ESEM) (Mark FEI Quanta 200) to see the effect of chemical activation with phosphoric acid on the structure of the raw material.

II.3. Batch mode biosorption studies

Removal of Pb(II), Cu(II), and Cd(II) ions onto the biosorbent was carried out by batch method and the influence of various parameters such as effect of pH, contact time, and biosorbent dose were studied. For each experimental run, 100 mL of metal solution of known concentration was taken in a 250 mL stoppered reagent bottle, pH was adjusted to the desired value by the addition of dilute aqueous solutions of HCl and NaOH, and a known amount of the biosorbent was added. This mixture was agitated at room temperature (25 °C) using a mechanical shake at a constant rate of 250 rpm for a prescribed time to attain equilibrium. At the end of the predetermined time intervals, the sample was taken out and the supernatant solution was separated from the biosorbent through polytetrafluoroethylene syringe filters (pore siz 0.45 µm) and analyzed the concentration of each metal ion Pb(II), Cu(II), or Cd(II) remaining in solution using ZEENIT atomic absorption spectrophotometer. Effect of pH was studied over the range of 2.0–6.0. Effect of biosorbent dose was studied in the range of 0.01–0.07g of biosorbent in 100 mL of metal solution. Kinetics and effect of contact time on biosorption were determined at different time intervals over a range of 5–240 min. Biosorption isotherms were studied by varying the initial metal ions concentration from 10 to 70 mg/L. The amount of biosorbed metal ion per gram of biosorbent at equilibrium, qe (mg/g), and the removal percentage, (% removal), were calculated using the following equations:

$$q_e = \frac{(C_0 - C_e)V}{m} \qquad (5)$$

$$\%removal = \frac{(C_0 - C_e)}{C_0} \times 100 \qquad (6)$$

where C_0 and C_e are the initial and equilibrium concentrations of metal ion, (mg/L). V is the volume of metal ion solution (L) and m is the weight of biosorbent used (g).

II.4. Desorption studies

Assays were performed in two phases:
Phase 1 - Biosorption: 0.05 g of the biosorbent was placed in contact with 100 mL of a 50 mg/L Pb(II), Cu(II),or Cd(II) solution in a bath shaken at 250 rpm and 25°C. The pH was adjusted to 5.0 for all solutions during the biosorption period. The contact time of biosorption was maintained 120 min for all solutions to achieving biosorption equilibrium. The biosorbent saturated with Pb(II), Cu(II), or Cd(II) was then collected by filtration, washed with distilled water and placed in an oven for 12 h at 60°C. The liquid phases were analyzed by ZEENIT atomic absorption spectrophotometer.
Phase 2 - Desorption: the dry and saturated biosorbent with Pb(II), Cu(II), or Cd(II) was placed in contact with 100 mL of 0.1 M HCl for 6 h in an agitated bath at a temperature of 25 °C with stirring at 250 rpm. The liquid phases were filtered and analyzed by ZEENIT atomic absorption spectrophotometer [12]. The performance of HCl in the biosorbent regeneration was examined in three biosorption - desorption cycles for all metal ions to determine the biosorbent regeneration. The initial and final metal concentrations of the solutions were recorded for each cycle. After each cycle of biosorption–desorption, the biosorbent thoroughly washed with deionized distilled water to neutrality and reconditioned for biosorption in

the succeeding cycle. The desorbed percentage was determined according to Equation (7).

$$\%\ \text{Desorbed} = \frac{\text{Amount desorbed ions}}{\text{Amount biosorbed ion}} \times 100 \quad (7)$$

II.5. Biosorption isotherm models

The biosorption equilibrium data of metal ions onto the biosorbent were analyzed in terms of Langmuir and Freundlich isotherm models [13] and also in terms of Dubinin–Radushkevich (D–R) and Temkin isotherm models [14] for the purpose of interpolation and limited extrapolation of the data. The relative coefficients of these models were calculated using least-squares fitting. Langmuir model is based on the assumption that biosorption energy is constant and independent of surface coverage. The maximum biosorption occurs when the surface is covered by a monolayer of adsorbate. The Langmuir isotherm is given by Eq. (8):

$$q_e = \frac{Q_m b C_e}{1 + bC_e} \quad (8)$$

The linear form of Langmuir isotherm equation is given as:

$$\frac{C_e}{q_e} = \frac{1}{Q_m b} + \frac{C_e}{Q_m} \quad (9)$$

where C_e is the equilibrium concentration of the adsorbate (mg/L), q_e is the amount of adsorbate adsorbed per unit mass of adsorbent (mg/g), b is the Langmuir adsorption constant (L/mg), and Q_m is the theoretical maximum adsorption capacity (mg/g).

The essential characteristics of the Langmuir isotherm can also be expressed in terms of a dimensionless constant of separation factor or equilibrium parameter, R_L, which is defined as

$$R_L = \frac{1}{(1 + bC_0)} \quad (10)$$

where b is the Langmuir constant and C_0 is the initial concentration of metal ions. The R_L value indicates the shape of isotherm [15]. R_L values between 0 and 1 indicate favorable adsorption, while R_L >1, R_L = 1, and R_L = 0 indicate unfavorable, linear, and irreversible adsorption isotherms.

Freundlich isotherm describes the heterogeneous surface energies by multilayer adsorption and is expressed in linear form as:

$$\log q_e = \log K_F + \left(\frac{1}{n}\right) \log C_e \quad (11)$$

The constants K_F (mg/g (L/mg) $^{1/n}$) and n of the Freundlich model are those indicative of the relative adsorption capacity of the adsorbent and the intensity of the adsorption, respectively. For values in the range 1< n < 10, adsorption is favorable [16].

Temkin isotherm based on the heat of adsorption of the ions, which is due to the adsorbate and adsorbent interactions taken in linear form, is given by

$$q_e = \left(\frac{RT}{b_T}\right) \ln A + \left(\frac{RT}{b_T}\right) \ln C_e \quad (12)$$

where B =RT/b_T, b_T is the Temkin constant related to the heat of sorption (J/mol), A is the Temkin isotherm constant (L/g), R the gas constant (8.314 J mol^{-1} K^{-1}) and T the absolute temperature (K).

Dubinin–Radushkevich (D–R) isotherm approach assumes that there is a surface area where the adsorption energy is homogeneous. The linear form of Dubinin–Radushkevich isotherm equation can be expressed as

$$\ln q_e = \ln Q_s - B\varepsilon^2 \quad (13)$$

where Q_S is the theoretical monolayer saturation capacity (mg/g), B is the Dubinin–Radushkevich

model constant (mol^2/kJ^2), and is the Polanyi potential and is equal to

$$\varepsilon = RT \ln\left(1+\frac{1}{C_e}\right) \qquad (14)$$

The mean energy of sorption, E (kJ/mol), is related to B as

$$E = \frac{1}{\sqrt{2B}} \qquad (15)$$

II.6. Biosorption kinetics models

In order to analyze the biosorption kinetics of metal ions onto the biosorbent, two kinetic models; pseudo-first-order and pseudo-second-order kinetic were applied for the experimental data. The pseudo-first-order equation can be expressed as [13]:

$$\log(q_e - q_t) = \log q_e - \frac{K_1}{2.303}t \qquad (16)$$

where qe and qt are the amounts adsorbed at equilibrium and at time t (mg/g), and k_1 is the rate constant of the pseudo-first-order adsorption (min^{-1}). The adsorption rate constant k_1, can be calculated by plotting $\log(q_e–q_t)$ versus t.

The pseudo-second-order kinetic model can be represented in the following form:

$$\frac{t}{q_t} = \frac{1}{K_2 q_e^2} + \frac{1}{q_e}t \qquad (17)$$

where k_2 (g/mg min) is the rate constant of second-order adsorption. k_2 and q_e can be obtained from the intercept and slope of plotting t/ q_t versus t.

III. RESULTS AND DISCUSSION

III.1. Characterization of the biosorbent

III.1.1. Physical characteristics

Surface area, porosity, pore volume and iodine number are characteristic parameters of the performance of the biosorbent.

The specific surface area of the biosorbent was estimated using the methylene blue biosorption method. The initial points on the isotherm plot of q versus C_e for the biosorption of MB on the biosorbent lie on the y-axis since the biosorbent at low initial solute concentration (100–200 mg/L) biosorbed all MB present in the solution (Fig. 1a). The plot of C_e/q versus C_e for the biosorption of MB on the biosorbent for initial MB solution concentrations ranging from 300 to 1000 mg/L at 25 °C gave a straight line with correlation coefficient 0.999 (Fig. 1b). The saturation biosorption amount was determined from the slope of the plot (Q_m = 125 mg/g). The specific surface area of the biosorbent was calculated as 306.25 m^2/g.

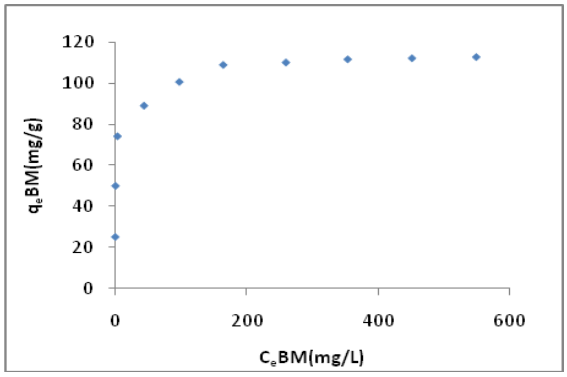

Fig. 1a. Biosorption isotherm of methylene blue on the biosorbent

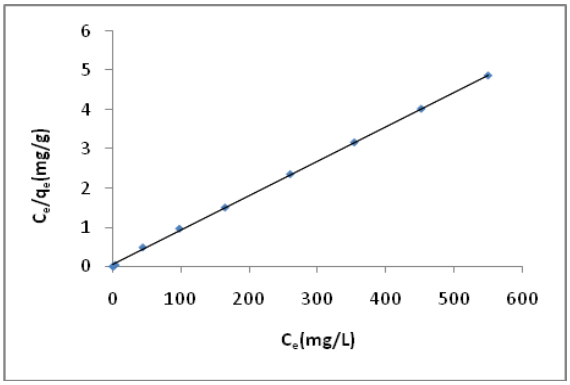

Fig. 1b. linear plot of langmuir isotherm for the biosorption of methylene blue on the biosorbent

The values of various physical parameters determined for the prepared biosorbent are regrouped in table I.

Table I. Physical parameters of the biosorbent

Physical parameters	Value
Estimated specific surface area (m^2/g)	306
Pore volume (cm^3/g)	0.88
Prosity (%)	69
Iodine number (mg/g)	846

The analysis of results presented in Table .I, can show that the developed biosorbent present a high iodine number which reveals their microporous structure.

The observation of the SEM image of the raw material (Fig. 2a) shows that the grains are not homogeneous with almost total absence of porosity. The external surfaces of the prepared biosorbent (Fig. 2b) show large cavities and are very irregular, indicating that the porosity of the material was produced by attack of the reagent (H_3PO_4) during activation.

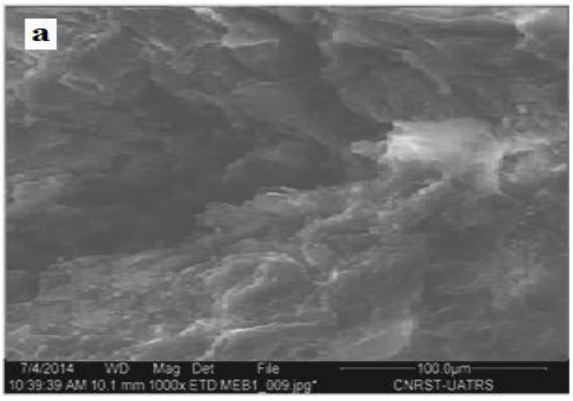

Fig. 2a. SEM images of raw material

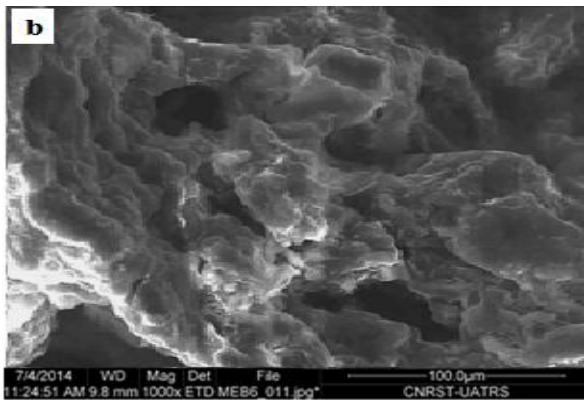

Fig. 2b. SEM images of biosorbent

III.1.2. Chemical characteristics

FTIR spectroscopic analysis: In this work, infrared spectroscopy was used to obtain information about the chemical structure and functional groups of the biosorbent (figure not shown). A wide absorption band at 3200–3600 cm^{-1} with a maximum at about 3400 cm^{-1} is assigned to O–H stretching vibrations of hydrogen bonded hydroxyl groups [17]. The absorption band at 2990 cm^{-1} is assigned to the stretching vibrations of aliphatic CH, CH2, and CH3 side chain groups of the aromatic nuclei. The absorption peaks at 2350 and 2330 cm^{-1} appeared for the biosorbent is possibly attributed to stretching [18]. The FTIR spectrum of the biosorbent contains absorbance peaks at 1600 and 1700 cm^{-1} which are the characteristics of C=O in quinone [19] and carboxylic acid structure respectively. The medium absorption band at 1400 cm^{-1} shows an aromatic ring of the biosorbent. The bands at 1200–1000 cm^{-1} have been assigned to C–O stretching vibrations in alcohols and phenols confirming the OH group in the biosorbent. The biosorbent contains –OH and C=O functional groups which could be involved in chemical bonding and may be responsible for the biosorption [20]. The oxygen of each carbonyl and hydroxyl group is considered a strong Lewis base because of the presence of nonbonding electron pairs. The oxygen base makes

coordination bonds with the metal ions (which are Lewis acids).

Oxygen functional groups: The identification and quantification of the surface oxygen groups in the biosorbent was done by means of the point of zero charge and Boehm titration. The results are detailed in table II.

The results show that the biosorbent produced by chemical activation is characterized by an acidic surface. The pH of the biosorbent was measured as 4.75. This result confirmed the Boehm analysis.

Table II. Chemical parameters of the biosorbent from Boehm method, pH, and Point of zero charge.

Chemical parameters	Value
Total of acid functions	1.34
Carboxylic (–COOH)	0.73
Lactones (–COO–)	0
Phenol (–OH)	0.61
Total of basic functions	0.295
pH	4.75
pH_{PZC}	4.25

X-Ray Diffraction Analysis: The X-Ray Diffraction pattern of the biosorbent (figure not shown) exhibit broad peaks and absence of a sharp peak that revealed predominantly amorphous structure, which is an advantageous property for well-defined biosorbents [21]. However, the occurrence of broad peak around 24° showed sign of formation of a crystalline carbonaceous structure, resulting in better layer alignment [22].

III.2. Biosorption proprieties

III.2.1. Effect of operating parameters

Effect of pH: The interaction between the metal ions and the functional groups of the biosorbent depends on nature of the biosorbent as well as on solution chemistry of the adsorbate, which in turn depends on pH of the solution [23] considerably influencing metal speciation, sequestration, and/or mobility [24-26]. Therefore, the effect of hydrogen ion concentration was examined using solutions in the pH range of 2.0–6.0. Fig. 3 summarizes the removal of Pb(II), Cu(II), and Cd(II) by the biosorbent as a function of pH. It is observed that the lead biosorption exhibits a higher dependence on pH while Cd(II) and Cu(II) have a similar profile with a slight dependence on pH. The removal of metal ions increased with increasing solution pH, reaching an optimum value at pH 5.0 for all studied metal ions. The lower removal of the studied metal ions at below optimum pH values can be attributed to effective competition between higher concentration of H^+ or H_3O^+ and metal ions present in the forms of M^{2+} and $M(OH)^+$ according to their (Pb, Cu and Cd) speciation diagrams [27-29]. The increase in metal removal as pH increased can be explained on the basis of a decrease in competition between proton (H^+ or H_3O^+) and positively charged metal ions [M^{2+} and $M(OH)^+$] at the surface sites. Also as pH increased surface positive charge of the biosorbent decreased which resulted in lower repulsion of the biosorbing metal ions. The pH_{PZC} of the biosorbent was 4.25, indicating negatively charged surface sites of the biosorbent at pH higher than 4.25. The optimum pH values for Pb(II), Cu(II), and Cd(II) were much higher than pH_{PZC} of the 4.25 (Fig. 3). At optimum pH values surface functional groups of the biosorbent may dissociate, by deprotonation resulting in negatively charged functional groups. Consequently, such negatively charged groups were showing affinity towards the positively charged or neutral metal species due to electrostatic interaction which may be responsible for the significant removal of metal ions by the following possible reactions [30].

$$R-OH+OH^- \leftrightarrow R-O^- + H_2O$$

$$R-O^- + M(II)X \leftrightarrow R-O^-M(II)X$$

When the pH was higher than the optimum pH (beyond the pH value of 5.0 for studied metal ions (Fig. 3) the metal ions may get converted to their hydroxides, and this resulted in a decrease in the removal of metals by the active sites of the biosorbent [29, 31-33]. Further, the biosorption process of metals by the biosorbent is kinetically faster than the precipitation of metal hydroxides under higher pH. The precipitation of metal hydroxide into the pores or spaces around the particles is hardly possible. Moreover, the percentage removal of metal ion was much greater by biosorption than by precipitation [33].

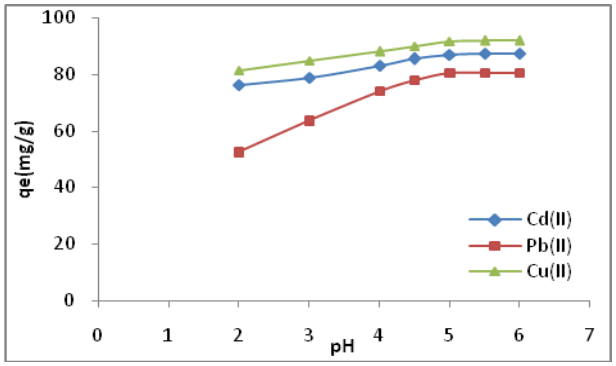

Fig. 3. Effect of pH on the biosorption of metal ions by the biosorbent at temperature =25 °C, contact time = 120min, metal ions initial concentration =50 mg/L, biosorbent dose =0.5 g/L and agitation speed =250 rpm.

Effect of biosorbent dose: Dosage study is an important parameter in biosorption studies because it determines the capacity of biosorbent for a given initial concentration of metal ion solution. The effect of biosorbent dose on the percent removal of Cu(II), Cd(II) and Pb(II) at initial concentration of 50 mg/L is shown in figure 4. From the figure it can be observed that increasing of biosorbent dose increased the percent removal of Cu(II), Cd(II) and Pb(II) up to 92.24, 87.75 and 80.53%, respectively, with the required optimum dosage of 0.5 g/L. Beyond the optimum dosage the removal efficiency did not change with the biosorbent dose. As expected, the removal efficiency increased with increasing the biosorbent dose for a given initial metal concentration. Indeed, for a fixed initial adsorbate concentration increasing biosorbent dose provides greater surface area or more biosorption sites. Further, it can be attributed to the binding of metal ions onto the surface functional groups present on the biosorbent.

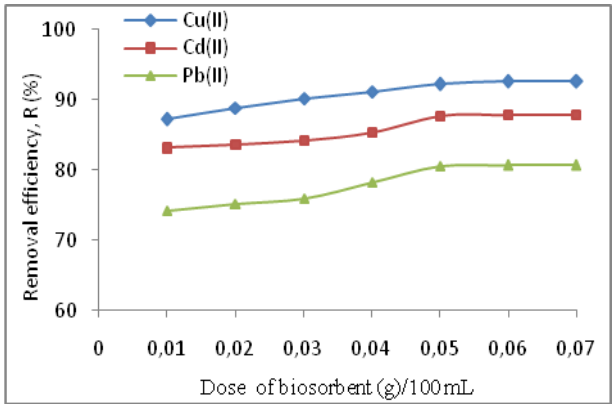

Fig. 4. Effect of biosorbent dose on the biosorption of metal ions by the biosorbent at temperature =25 °C, contact time =120 min, metal ions initial concentration =50 mg/L, pH =5 and agitation speed =250 rpm.

Effect of contact time: Equilibrium time is one of the important parameters for an economical wastewater treatment system [34]. The experimental results relating to the effect of contact time on removal of Pb(II), Cu(II), and Cd(II) are shown in figure 5. The kinetic curves of the three metal ions show that the equilibrium is quickly established for all biosorbates. In fact these curves present similar speeds and each of them corresponds to a rapid increase in the amount adsorbed which is fixed after 30 min for Cu(II), Cd(II), and Pb(II) with concentration of 93 mg/L, 88 mg/L and 80 mg/L onto the biosorbent respectively.

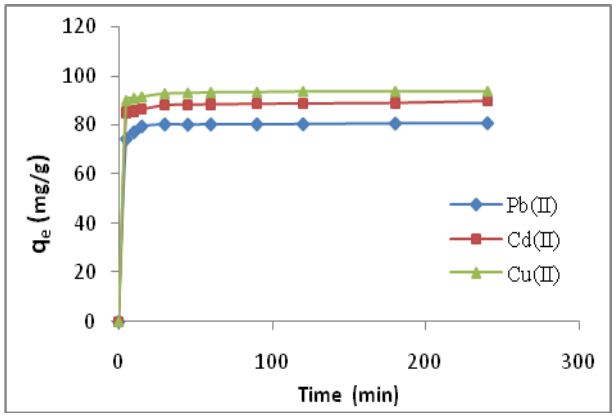

Fig.5. Effect of contact time on the biosorption of metal ions by the biosorbent at temperature =25 °C, biosorbent dose =0.5 g/L, metal ions initial concentration =50 mg/L, pH=5 and agitation speed =250 rpm.

III.2.2. Biosorption isotherms

The relationship between the amount of a substance adsorbed per unit mass of biosorbent at constant temperature and its concentration in the equilibrium solution is called the biosorption isotherm. The equilibrium biosorption isotherms are important in determining the biosorption capacity of metal ions Cu(II), Cd(II), and Pb(II) and diagnose the nature of biosorption onto the biosorbent. The biosorption data were fitted to Langmuir, Freundlich, Dubinin–Radushkevich, and Temkin biosorption isotherm models described in Section II.5. As can be seen from the regression coefficients in table III, the Langmuir model show the best fit compared to Freundlich, Temkin, and Dubinin–Radushkevich models. The maximum loading capacities of the biosorbent was obtained as 333.33 mg/g for Cu(II), 250 for Cd(II), and 200 mg/g for Pb(II), so the ability of Cu(II) biosorption on the biosorbent is bigger than Cd(II) and Pb(II). The dimensionless parameter (R_L) value, which is edefined in Eq. (10) described above can be computed by substituting the values of b and C_0 to the equation. The R_L values were 0.23 for Cu(II), 0.24 for Cd(II), and 0.31 for Pb(II). For the three metal ions the values of R_L were between 0 and 1, pointing out the favorable biosorption onto the biosorbent [15]. Freundlich coefficient K_f , which represents the biosorption capacity was found to be increased in the sequence, Pb(II) < Cd(II) < Cu(II) (Table III). The other Freundlich coefficient "n" values fulfilled the condition of 0 < n < 10 for favorable biosorption. The Langmuir type biosorption isotherm is an indication of surface homogeneity of the biosorbent. Compared to other biosorbents, the adsorptive capacity of Cu(II), Cd(II) and Pb(II) biosorption on the biosorbent is better than others biosorbents (Table IV).

Table III: Constants of Langmuir, Freundlich, szDubinin–Radushkevich, and Temkin isotherm models for Cu(II), Cd(II) and Pb(II) biosorbed by the biosorbent.

Model	Metal ion		
	Cu(II)	Cd(II)	Pb(II)
Langmuir isotherm			
Qm (mg/g)	333.33	250	200
b (l/mg)	0.107	0.105	0.071
R_L	0.234	0.237	0.308
R^2	0.997	0.997	0.998
Freundlich isotherm			
K_F(mg/g)	33.27	27.48	15.14
$l/mg)^{1/n}$	1.39	1.58	1.38
n	0.994	0.995	0.989
R^2			
Temkin isotherm			
b_T (J/mol)	46.66	55.91	68.23
A (L/g)	1.50	1.26	0.98
R^2	0.988	0.989	0.976
Dubinin-Radushkevich isotherm			
Q_S (mg/g)	97.03	88.68	79.60
$B_* 10^{-7}$	3	4	9
E (kJ/mol)	1291	1118	745.35
R^2	0.882	0.868	0.852

Table IV: Comparison of biosorption capacity of the biosorbent with recently reported biosorption studies of biomass materials for the removal of Cu(II), Cd(II) and Pb(II).

Table IV: Comparison of biosorption capacity of the biosorbent with recently reported biosorption studies of biomass materials for the removal of Cu(II), Cd(II) and Pb(II).

Biomass material	Metal	Biomasse type	Biosorption capacity (mg /g)	References
Sargassum vulgare	Cd	Algae	250	This study
Cinachyrella tarentine	Cd	Sponge	166.67	[7]
Spirulina sp.	Cd	Bacteria	99.5	[35]
Ulva onoi	Cd	Algae	90.7	[36]
Azolla filiculoides	Cd	Plants	111-132	[37]
Sargassum vulgare	Pb	Algae	200	This study
Cinachyrella tarentine	Pb	Sponge	142.86	[7]
Saccharomyces cerevisiae	Pb	Fungi (yeast)	85.6	[38]
Streptomyces rimosus	Pb	Bacteria	135	[39]
Spirodela polyrhiza **(L.)**	Pb	Aquatic plant	137	[40]
Sargassum vulgare	Cu	Algae	333,33	This study
Cinachyrella tarentine	Cu	Sponge	166.67	[7]
Sphaerotilus natans	Cu	Bacteria	60	[41]
Acrylic acid functionalized poly hydrogel	Cu	Biomass based material	67.25	[42]
Spirulina sp.	Cu	Bacteria	196	[35]

III.2.3. Biosorption kinetics

The prediction of kinetics is necessary for the design of biosorption systems. Measurement of biosorption rate constants and order of the reaction are important physico-chemical parameters to evaluate the basic qualities of a good adsorbent. In order to observe the biosorption process of Cu(II), Cd(II) and Pb(II) ions onto the biosorbent, pseudo-first-order and pseudo-second-order kinetic models which are described in earlier Section II.6 were implemented. The pseudo-second-order plots (figure not shown) for the removal of Cu(II), Cd(II) and Pb(II) by the biosorbent were used to calculate the three rate constants k_2 and biosorption capacities q_e. In the same manner, the pseudo-first-order plots (figure not shown) for the removal of Cu(II), Cd(II) and Pb(II) by the biosorbent were used to calculate the three rate constants k_1. The biosorption rate constants (k_1 and k_2) and biosorption capacity (q_e) for the removal of metal ions by the biosorbent are thus reported in table V. Since the correlation coefficients are consistent and equal to unity for pseudo-second-order kinetic model than for pseudo-first-order kinetic model, besides the experimental q_e values did not agree with the calculated values obtained from the linear pseudo-first-order plots (Table V). This indicating that the biosorption kinetics can be well explained by pseudo-second-order kinetic model for the removal of Cu(II), Cd(II) and Pb(II) by the biosorbent.

Table V: Pseudo-first-order and pseudo-second-order kinetic model for removal of Cu(II), Cd(II) and Pb(II) by the biosorbent

Modèle cinétique	Metal ion		
	Cu(II)	Cd(II)	Pb(II)
q_e . exp (mg/g)	93.68	89.46	80.75
Pseudo-first-order			
q_e. cal (mg/g)	3.01	3.25	2.3
K_1 (min^{-1})	0.02	0.01	0.01
R^2	0.97	0.757	0.751
Pseudo-second-order			
q_e. cal (mg/g)	100	90.91	83.33
K_2 (g mg^{-1} min)	0.03	0.01	0.02
R^2	1	1	1

III.2.4. Desorption studies

Desorption studies help the recovery of the metal from waste and the regeneration of the adsorbent to decide its potential as an adsorbent for

commercial application. The use of thermal activation to regenerate the adsorbent could require high energy and adsorbent loss in each cycle. Hence, studies were carried out to use chemical regeneration for adsorbate desorption. Desorption studies were carried out using HCl (0.1M) solution, which has been reported to be an efficient metal desorbent [43]. The capacity of the biosorbent to adsorb Cu(II), Cd(II) and Pb(II) was determined by repeating the biosorption experiments in three consecutive cycles. As illustrated in table VII, the biosorbent undergoing successive biosorption–desorption processes retained good metal biosorption capacity even after 3 cycles and higher than 95% desorption was obtained after three-biosorption–desorption cycles. The total decrease in biosorption efficiency the biosorbent for Cu(II), Cd(II) and Pb(II) after three cycles were 6,2%, 6,55% and 1,81%, respectively, which showed that the biosorbent had good potential to adsorb metal ions repeatedly from aqueous solution.

Table VII: Biosorption and desorption of heavy metal ions by the biosorbent in three consecutive cycles

Cycle No	Metal biosorbed **(mg/g)**			**Métal** desorbed **(%)**		
	Cu(II)	**Cd(II)**	**Pb(II)**	**Cu(II)**	**Cd(II)**	**Pb(II)**
1	92.32	87.96	80.64	95.43	99.00	98.64
2	89.20	85.53	79.94	96.78	98.39	99.11
3	86.59	82.19	79.18	95.53	97.77	98.74

CONCLUSION

In this study, we developed a new biosorbent from the extract residue of the marine alga *Sargassum vulgare* by chemical activation with phosphoric acid. The functional groups on the surface of the biosorbent such as phenolic hydroxyls and carbonyl groups that were formed during the activation process played effective role in the removal of heavy metal ions. Biosorption process was affected by experimental parameters such as pH, contact time, and biosorbent dosage. The optimum pH values for Cu(II), Cd(II) and Pb(II) were much higher than pH_{PZC} of the 4.25, which suggest that the metallic species uptake may be related to the electrostatic interaction of the metal species with the negatively charged functional groups on the biosorbent surface. Biosorption of Cu(II), Cd(II) and Pb(II) on the biosorbent was found to follow a pseudo-second order kinetic model. Biosorption isotherms were better described by Langmuir model in comparison to Freundlich, Temkin and Dubinin–Radushkevich models. Thus these studies revealed that the prepared biosorbent, can be effectively used as an effective biosorbent for the removal of heavy metals from water and wastewater.

References

[1] Matei G.M., Kiptoo J.K., Oyaro N. and Onditi A. O. Biosorption of Selected Heavy Metals by Green Algae, Spirogyra Species and Its Potential as a Pollution Biomonitor. Chem. Mat. Res. 2015.7 (7).p.42-52

[2] Nabi S.A., Bushra R., Al Othman Z.A., Naushad Mu., Synthesis, characterization, and analytical applications of a new composite cation exchange material acetonitrile stannic (IV) selenite: adsorption behavior of toxic metal ions in non ionic surfactant medium. Sep. Sci. Technol.) 2011. 46(5).p.847-857.

[3] Babarinde N. A. A., Babalola J. O., Sanni R. A. Biosorption of lead ions from aqueous solution by maize leafInt. J. Phys. Sci. 2006. 1. p. 23–26.

[4] Klimmek, S., Stan, H.J., Wilke, A., Bunke, G., Buchholz, R. Comparative analysis of the biosorption of cadmium, lead, nickel and zinc by algae. Environ. Sci. Technol. 2001. 35. p.4283–4288.

[5] Tarbaoui M., Oumam M., Fakhfakh N., Charrouf M., Berrada M., Bennamara A., Abourriche A.. Optimization of conditions for the preparation of new adsorbent material from residues of marine algae applying a response surface methodology. IOSR-JAC. 2014. 7(10). p. 76-86.

[6] Benzina M., Bellagi A. Détermination des propriétés du réseau poreux de matériau argileux par les techniques d'adsorption d'azote et de porosimétrie au mercure en vue de leur utilisation pour la récupération des gaz. Anal. Chim. 1990. 15. p.315-335.

[7] Tarbaoui M., Oumam M., El Amraoui B., Bennamara A., Benzina M., Fourmentin S., Abourriche A. Biosorption and desorption of lead, copper and cadmium ionsby a new material prepared from the marine sponge Cinachyrella tarentina. J. Mater. Environ. Sci. 2015. 6 (11).p. 3281-3294.

[8] Demiral H., Demiral I., Karabacakoglu B., Tumsek F. Production of activated carbon from olive bagasse by physical activation. Chem. Eng. Res. Des. 2011. 89. p.206-213.

[9] Bouzid J., Elouear Z., Ksibi M., Feki M., Montiel A. A study on removal characteristics of copper from aqueous solution by sewage sludge and pomace ashes. J. Hazardous. Mater. 2008. 152. p.838–845.

[10] Starck J., Burg P., Cagniant D., Tascon J. M. D., Martinez-Alonso A., The effect of demineralisation on a lignite surface properties. Fuel. 2004. 83. p.845–850.

[11] Boehm H.P. Some aspects of the surface chemistry of carbon blacks and other carbons. Carbon. 1994. 32. p.759–769.

[12] Cechine M. A. P., Ulson de Souza S. M. A.G., Ulson de Souza A. A. Study of lead (II) adsorption onto activated carbon originating from cow bone. J. Clean. Prod. 2014. 65.p. 342-349

[13] Purna C. R. G., Satyaveni S., Ramesh A., Seshaiah K., Murthy K. S. N., Choudary N.V. Sorption of Cadmium and Zinc from Aqueous Solutions by Zeolite 4a, Zeolite 13x and Bentonite. J. Environ. Manage. 2006. 81. p. 265–272.

[14] Kundu S., Gupta A. K.. Regression analysis of equilibrium data with several isotherm models and their optimization. Chem. Eng. J, 2006. 122. p. 93–106.

[15] Mckay G., Blair H. S., Gardener J. R. Adsorption of dyes on chitin. I. Equilibrium studies. J. Appl. Polym. Sci. 1982. 27. p. 3043–3057.

[16] Raji C., Anirudhan T. S. Batch Cr(VI) removal by polyacrylamide-grafted sawdust: Kinetics and thermodynamics. Water. Res. 1998. 32. p.3772–3780.

[17] Valente N. J. M., Laginhas C. E. C., M. M. L Carrott,. Ribeiro Carrott. Production of activated carbons from almond shell. Fuel. Process. Technol. 2011. 92. p.234–240.

[18] Jia Y. F., Xiao B., Thomas K. M.. Adsorption of metal ions on nitrogen surface functional groups in activated carbons, Langmuir. 2002. 18. 470–478.

[19] Tsai W. T., Chang C. Y., Lin M. C., Chien S. F., Sun H. F., Hsieh M. F. Adsorption of acid dye onto activated carbons prepared from agricultural waste bagasse by $ZnCl_2$ activation. Chemosphere. 2001. 45. p.51-58.

[20] Ho Y. S., Removal of copper ions from aqueous solution by tree fern, Water. Res. 2003. 37. p. 2323–2330.

[21] Omri A., Benzina M., Ammar N.. Preparation, modification and industrial application of activated carbon from almond shell. J. Ind. Eng. Chem. 2013. 19. p.2092-2099.

[22] Kennedy L. J., Vijaya J. J., Kayalvizhi K., Sekaran G. Adsorption of phenol from aqueous solutions using mesoporous carbon prepared by two-stage process. Chem. Eng. J. 2007.132. p. 279-287.

[23] Bae W., Wu C. H., Kostal J., Mulchandani A., Chen W. Enhanced Mercury Biosorption by Bacterial Cells with Surface-Displayed MerR. Appl. Environ. Microbiol. 2003. 69. p.3176–3180.

[24] Merifield J. D., Davids W. G., MacRae J. D., Amirbahman A. Uptake of mercury by thiol-grafted chitosan gel beads. Water. Res. 2004. 38. p. 3132–3138.

[25] Kraemer S., Hering J. G. Biogeochemical controls on the mobility and bioavailability of metals in soils and ground water. Aquat. Sci. 2004. 66. p.1–2.

[26] Miretzky P., Bisinoti M. C., Jardim W. F., Rocha J. C. Factors affecting hg (ii) adsorption in soils from the rio negro basin (amazon). Quím. Nova. 2005. 28. p. 438–443.

[27] Elliott H. A., Huang C. P. Adsorption Characteristics of Some Cu(II) Complexes on Aluminosilicates. Water. Res. 1981. 15. p. 849–855.

[28] Li Y. H., Wang S., Wei J., Zhang X., Xu C., Luan Z., Wu D., Wei B. Lead adsorption on carbon nanotubes. Chem. Phys. Lett. 2002. 357. p. 263.

[29] Lu C., Chiu H. Adsorption of Zinc (II) from Water with Purified Carbon Nanotubes. Chem. Eng. Sci. 2006. 61. p.1138–1145.

[30] Das S. K., Das A. R., Guha A. K.. A study on the adsorption mechanism of mercury on Aspergillus versicolor biomass. Environ. Sci. Technol. 2007. 41. p.8281–8287.

[31] Shanmugavalli R., Syed Shabudeen P. S., Venckatesh R., Kadirvelu K., Madhavakrishnan S., Pattabhi S. Uptake of Pb (II) ion from Aqueous Solution Using Silk Cotton Hull Carbon: An Agricultural Waste Biomass. E-J. Chem. 2006. 3. p. 218–229.

[32] Sar P., Kazy S.K., Asthana R.K., Singh S.P. Metal adsorption and desorption by lyophilized Pseudomonas aeruginosa. Int. Biodeter. Biodegr. 1999. 44. p. 101–110.

[33] Namasivayam C., Ranganathan K.. Removal of Cd(II) from wastewater by adsorption on "waste" Fe(III)/Cr(III) hydroxide. Water. Res. 1995. 29. p. 1737–1744.

[34] Kadirvelu K., Namasivayam C. Activated carbon from coconut coirpith as metal adsorbent: adsorption of Cd(II) from aqueous solution. Adv. Environ. Res. 2003. 7. p.471–478.

[35] Chojnacka K., Chojnacki A., Gorecka H., Biosorption of Cr^{3+}, Cd^{2+} and Cu^{2+} ions by blue-green algae. Chemosphere. 2005. 59. p.75–84.

[36] Suzuki Y., Kametani T., Maruyama T. Removal of heavy metals from aqueous solution by nonliving Ulva seaweed as biosorbent. Water. Res. 2005. 39. p. 1803–1808.

[37] Rakhshaee R., Khosravi M., Ganji M. T. Kinetic modeling and thermodynamic study to remove Pb(II), Cd(II), Ni(II) and Zn(II) from aqueous solution using dead and living Azolla filiculoides. J. Hazard. Mater. 2006. 134. p. 120–129.

[38] Chen C., Wang J. Influence of metal ionic characteristics on the biosorption capacity by *Saccharomyces cerevisiae*. App. Microbiol. Biotechnol. 2007. 74. p. 911–917.

[39] Selatnia A., Boukazoula A., Kechid N., Bakhti M. Z., Chergui A., Kerchich Y. Biochem. Biosorption of lead (II) from aqueous solution by a bacterial dead Streptomyces rimosus biomass. Eng. J. 2004. 19. p. 127–135.

[40] Meitei M. D., Prasad M. N. V. Lead(II) and cadmium(II) biosorption on Spirodela polyrhiza (L) Schleiden biomass. J. Environ. Chem. Eng. 2013. 1. p.200–207.

[41] Beolchini F., Pagnanelli F., Toro L., Veglio F. Ionic strength effect on copper biosorption by Sphaerotilus natans: equilibrium study and dynamic modelling in membrane reactor. Water. Res. 2006. 40. p. 144–152.

[42] Chen J. J., Ahmad A. L., Ooi B. S., Poly(N-isopropylacrylamide-co-acrylic acid) hydrogels for copper ion adsorption: Equilibrium isotherms, kinetic and thermodynamic studies. J. Environ. Chem. Eng. 2013. 1. p.339–348.

[43] Saeed A., Iqbal M., Bioremoval of cadmium from aqueous solution by black gram husk (Cicer arientinum). Water. Res. 2003. 37. p. 3472–3480.